Gas sensitivity amplification of interdigitated chemocapacitors through etching

P. Oikonomou, A. Botsialas, N. Papanikolaou, I. Kazas, K. Ntetsikas, G. Polymeropoulos, N. Hadjichristidis, M. Sanopoulou, I. Raptis

Abstract—**In polymer coated planar Inter Digitated Electrodes (IDEs), the gas sensing sensitivity is much lower than the sensitivity of parallel plate capacitors. Here, we introduce a simple patterning step for the modification of the geometry of the dielectric substrate of the planar IDEs, and increase of the contribution of the sensitive layer to the output signal. The proposed methodology is investigated through simulation and verified by experimental data. Polymer coated IDEs with different dimensions of spatial wavelength were studied experimentally upon exposure to analytes of varying polarity. The sensing performance of the fabricated structures compare very well with theoretically estimated values obtained through finite element simulations. The maximum performance gain is also calculated by simulation demonstrating the potential of the technology.**

Index Terms—**Interdigitated Electrodes, chemocapacitors, microelectronic processing.**

I. INTRODUCTION

InterDigitated Electrodes (IDEs) have been proved a quite versatile platform for sensing applications. They offer several features that make them a suitable platform for implementation in a wide range of diverse applications. Their most important characteristics are: (a) the ease of realization with mainstream microelectronic processes that allow for volume production of miniaturized chips with high repeatability between chips on the same wafer substrate (either glass or silicon) and chips from different wafers (b) the realization of chips with arrays of IDEs electrically isolated that can be employed for multi-analyte determinations (c) facile measurement of the sensors' responses with commercially available electronic modules and (d) ultra-low power consumption. All these unique features make IDEs the ideal sensing platform for long term monitoring of gaseous environments provided that the sensor response is reversible and of low drift.

IDEs have been mainly explored for the detection of analytes in air focusing primarily on the detection of harmful or toxic substances [1-9] but research effort has been also directed towards the detection of Volatile Organic Compounds (VOCs) in soil and liquids [10-13]. In the applications related to the detection of analytes in air, IDEs are usually coated with polymeric materials with selective absorbance of particular analytes. The sorption of analyte's molecules, changes the dielectric constant of the polymeric coating that results in a capacitance change of the device that can be correlated to the concentration of the particular analyte [14]. In order to increase the capacitance change due to the sorption of analyte, several approaches have been explored. "Parallel plates" capacitors [15] offer higher analytical performance than planar IDEs capacitors, but their fabrication faces certain technological difficulties. In this case, the polymeric material must fill the tiny gap between the two electrodes while the top electrode has to be perforated to allow the interaction between the analyte-target and the sensing layer, limiting this way the surface available for interaction. In the case of planar IDEs, several theoretical studies about the optimization of the sensing performance have been reported [16-18] with shrinkage of the electrodes width being the dominant task that is performed with standard microelectronic processes [19].

In planar IDE structures, approximately half of the electric field lines pass through the polymeric coating, and the rest pass through the substrate. Given that the dielectric substrate (SiO_2 in most of the studies) is not altered in the presence of analytes, the sensor's response (capacitance change) [20-24] is approximately half of the maximum response (if the substrate would be of the same polymeric sensing material). This has a pronounced effect on the sensing performance of the device. In order to address this issue, we propose, the etching of the dielectric substrate as a simple yet reliable, repeatable and low-

cost approach for the amplification of the sensing performance. In this work, this approach is evaluated through simulation and experimentally verified.

Initially, the sensing performance of planar IDEs is evaluated with Finite Element Simulations by using COMSOL Multiphysics and then the sensing responses of the fabricated IDEs are compared with the simulation ones. Additionally, experimental measurements of chemocapacitors coated with synthesized, on-purpose, polymeric materials upon exposure to analytes of varying polarity, is performed.

II. MATERIALS & METHODS

A. Sensors Configuration

In Fig. 1 a typical top view illustration of the IDE layout employed in the present study is presented. The IDEs spatial wavelength is defined as $\lambda = 2(W+G)$, where W (μm) is the electrode width and G (μm) is the gap between the consecutive unevenly charged electrodes. The cross-section of the IDE structure coated with a polymeric layer (chemocapacitor) is illustrated in Fig. 2. In Fig. 2A the dielectric substrate of the IDE is planar (initial design) and in Fig. 2B it is anisotropically patterned with Reactive Ion Etching (RIE) without any distortion of the metal electrode dimensions [25].
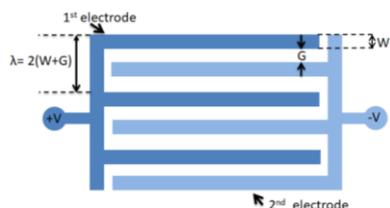

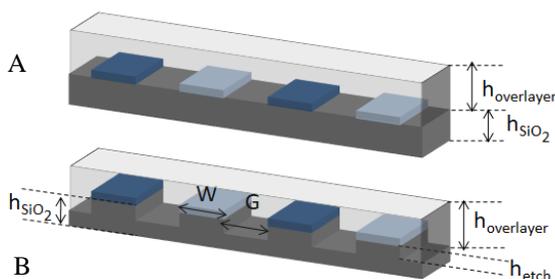Fig. 1. Simplified Schematic top view of InterDigitated Electrodes (IDEs).

Fig. 2. 3D illustration of the chemocapacitor, used in COMSOL simulations, without (A) and with (B) substrate patterning.

TABLE I
ABBREVIATIONS FOR IDES LAYOUTS STUDIED

IDEs configuration	Abbreviation [a]
IDEs with $\lambda=8$ μm, where W=1.0 μm and G=3.0 μm. The SiO2 substrate is not patterned.	1A
IDEs with $\lambda=8$ μm, where W=1.0 μm and G=3.0 μm. The etching depth in the SiO2 areas between the Al electrodes is 750 nm.	1B
IDEs with $\lambda=4$ μm, where W=1.3 μm and G=0.7 μm. The SiO2 substrate is not patterned.	2A
IDEs with $\lambda=4$ μm, where W=1.3 μm and G=0.7 μm. The etching depth in the SiO2 areas between the Al electrodes is 250 nm.	2B

In the present study, IDEs layouts with λ values of: a) 8μm, and b) 4μm were studied. In both cases the effect of the substrate's patterning to the sensitivity amplification is investigated. The actual geometrical characteristics are explained, along with an abbreviation in Table I.

The sensing area of each one of the two layouts has been designed in order to fulfill the specifications of the readout electronics modules (see next section).

B. Sensors Fabrication

The IDEs were fabricated with standard microelectronic/micromachining processing steps employing thermal oxidation, lithography and etching. In chips 1A and 1B, $\lambda=8$μm, the thickness of aluminum electrodes is approximately 300 nm and the sensing area is designed to be 0.90 mm^2. In chips 2A and 2B, the thickness of the Al electrodes is approximately 120 nm and the sensing area is designed to be 0.64 mm^2. The dimensions of the sensing areas were selected so that the capacitance before and after sorption is within the range (0–21 pF) of a miniaturized read-out electronics module [14], that allows for facile measurement of the sensor response and easy implementation in applications at the field. In Fig. 3 top view SEM images of IDEs from both layouts are illustrated.

After the realization of the IDE arrays, a reactive ion etching step follows in order to selectively etch the SiO$_2$ areas between the electrodes and produce the 1B and 2B chips. The etching step is performed in a Reactive Ion Etcher (Alcatel NE330) with the following conditions: RF Frequency: 13.5 MHz, RF Power: 400 Watt, chamber pressure: 10 mTorr and gas flow rate: 50 sccm Trifluoromethane (CHF$_3$).

Each chip accommodates 8 IDEs, all of them sharing the same layout. The interconnects end to contact pads of 0.04 mm^2 area, for facile wire bonding in a DIL package. The packaged IDE arrays are integrated with the readout electronic module that allows for the operation, control and data transfer to a PC or other unit with data storage and processing capabilities [14].
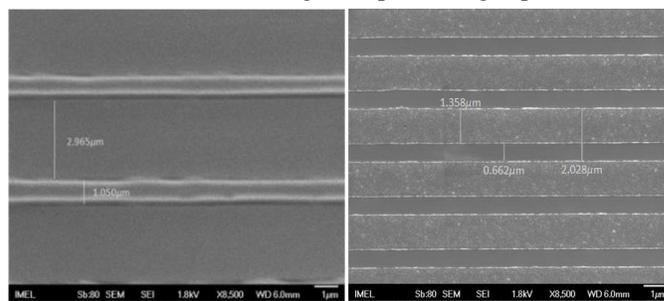
Fig. 3. Top view SEM images of IDEs. (A) 1A/1B chips and (B) 2A/2B chips

C. Synthesis of homo and copolymers

In the present work, polymers synthesized-on-purpose in the lab were employed as sensing layers for humidity and certain VOCs: non-polar solvent (Toluene), and a weakly-polar solvent (Ethyl Acetate, EtOAc). The selected polymeric materials are glassy Polystyrene (PS), elastomeric Polyisoprene (PI) and a copolymer of PI and PS, Tapered Poly(isoprene-tap-styrene) (PI-S)tap. In the case of rubbery polymers, organic solvent vapors can be absorbed by a dissolution process according to

the Flory-Huggins-type sorption mechanism. The sorption increases linearly at lower concentrations according to Henry's law [26] and the isotherm curves upwards rapidly in the higher concentration range. On the other hand glassy polymers, in addition to the dissolution mechanism of sorption, show excess sorption in the frozen microvoids of the glassy structure according to Langmuir's law (dual-mode sorption model) [27].

D. Materials & instrumentation for synthesis

Benzene (Sigma Aldrich, 99%) was purified over CaH_2 and distilled under high vacuum into a round bottom flask containing polystyrylithium oligomers [PS(-)Li(+)], exhibiting the characteristic yellow-orange color. sec-Butyllithium (Sigma-Aldrich, 1.4 M in cyclohexane) was diluted to the appropriate concentration in purified benzene, in a custom-made glass apparatus under high vacuum. Styrene (Sigma Aldrich, 99%) was purified by distillation over CaH_2 and dibutyl-magnesium (Sigma-Aldrich, 1 M solution in heptane) and stored in pre-calibrated ampoules. Isoprene (Sigma Aldrich, 99%) was purified over CaH_2 and subsequently by double distillation over n-BuLi where it remained under stirring for 30 min at 0 °C and finally stored in pre-calibrated ampoules. Methanol (Sigma-Aldrich, 99.8%) (terminating agent) was distilled over CaH_2 and stored under high vacuum.

TABLE II
MOLECULAR CHARACTERISTICS OF PS AND PI ([A] SEC IN THF AT 35 °C USING POLYSTYRENE STANDARDS

Samples	[A] Mn (g/mol)	[A] Đ
PS	101000	1.05
PI	120000	1.07

TABLE III
MOLECULAR CHARACTERISTICS OF TAPERED COPOLYMER OF ISOPRENE AND STYRENE ([A] SEC IN THF AT 35 °C USING POLYSTYRENE STANDARDS. [B] MASS FRACTION WAS CALCULATED BY ^{1}H-NMR SPECTROSCOPY IN $CDCL_3$ AT RT).

Sample	[a] Mn (g/mol)	[a] Đ	[b] f(PI) %(w/w)	[b] f(PS) %(w/w)
P(I-S)$_{tap}$	90000	1.10	0.45	0.55

E. Synthesis & characterization of Polymeric materials

All polymerizations were carried out by high vacuum techniques, using custom-made glass reactors, equipped with break-seals for the addition of the reagents and constrictions for the removal of aliquots [28].

The linear polystyrene was synthesized by anionic polymerization of styrene (5 g) initiated by 0.05 mmol sec-BuLi in benzene at RT in an evacuated and n-BuLi washed glass reactor. After 24 hours the reaction was quenched by addition of methanol (~1 mL) and the solution poured in a large excess of methanol to precipitate the polymer.

The synthetic procedure for the linear polyisoprene with high 1,4 microstructure, involves the anionic polymerization of isoprene (5 g) in benzene with 0.041 mmol of sec-BuLi at RT. After 24 hours, the polymerization quenched with methanol and the polymer precipitated in methanol.

The tapered (gradient) copolymer of styrene and isoprene was synthesized via anionic copolymerization of equimolar amounts (0.073 mmol) of styrene and isoprene in benzene at

room temperature, using sec-BuLi as initiator. The tapered structure of the copolymer is due to the big difference in the reactivity ratios of isoprene and styrene in a non-polar solvent [29]. The SEC traces and the ^{1}H-NMR spectra of all three polymers are given in the supplementary part while the molecular characteristics are given in Tables II and III.

III. SIMULATION

The capacitance of the IDEs was calculated using the COMSOL Multiphysics (www.comsol.com) finite element simulation package. In all cases the sensing layer height was set higher than $\lambda/2$ of the IDEs. According to Igreja and Dias [17, 30] the sensitivity increases with increasing the sensing film thickness because more field lines pass through the sensitive region, but it saturates as the film thickness approaches $\lambda/2$ of the IDEs. We used stationary electrostatics models to compute the capacitance, where one electrode was defined as ground and the other was given a 1 V terminal voltage.

In Fig. 4, the electric field profiles around the electrodes for the simulated structures of the four IDEs layouts, are presented. In the patterned dielectric substrates (1B, 2B respectively), the contribution of the overlayer in total capacitance is increased, while the substrate's contribution is reduced.
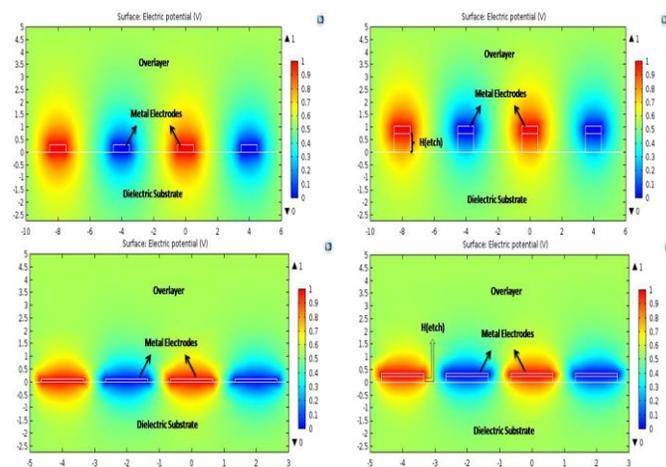

Fig. 4. Electric potential profile around the electrodes obtained through simulation for 1A, 1B, 2A and 2B IDEs layouts. Axes show dimensions in μm. The lateral dimensions of the device under simulation are 65 * 85 μm² and the thickness of the substrate and of the overlayer is 5 μm. The layer stack consists of: (a) SiO₂ (ε=3.9) as substrate, (b) 300 nm or 120 nm thick Al as electrodes (ε= 10.0) and (c) overlayer of polymeric film (ε_r in the 1.0–6.0 range) or air (ε= 1.0).

The effect of the etching depth on the total capacitance and on the capacitance change is illustrated in Figs. 5 and 6 where the calculated capacitance for varying overlayer permittivity (ε_r) for the four structures under study is presented. In all cases capacitance varies linearly with ε_r. The sensitivity is defined by the ratio $\Delta C/\Delta\varepsilon_r$, with $\Delta C = C - C_{air}$, where C_{air} is the capacitance for air ($\varepsilon_r = 1$) as overlayer, and C is the capacitance for overlayer with dielectric constant values larger than that of air. The ratio $\Delta C/\Delta\varepsilon_r$ determines the capacitance change for a unit change in the sensing film's permittivity. In order to compare the sensing performance between the various layouts, the quantity ($\Delta C/C_{air})/\Delta\varepsilon_r$, is introduced, since the uncoated capacitance (C_{air}) depends on both the layout and the patterning.
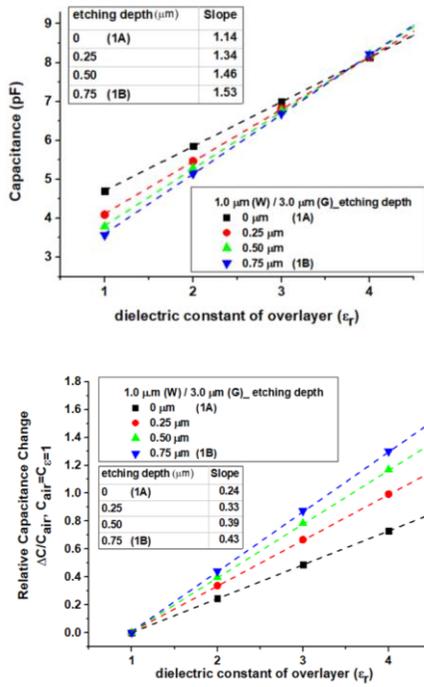
Fig. 5. Simulation data for IDEs with W= 1.0 μm and G= 3.0 μm with aluminum thickness of 300 nm without etching (configuration 1A) and various etching depth values as described in the inset (configuration 1B is included). (A) Capacitance vs. dielectric constant of overlayer and (B) relative capacitance change vs. dielectric constant of overlayer
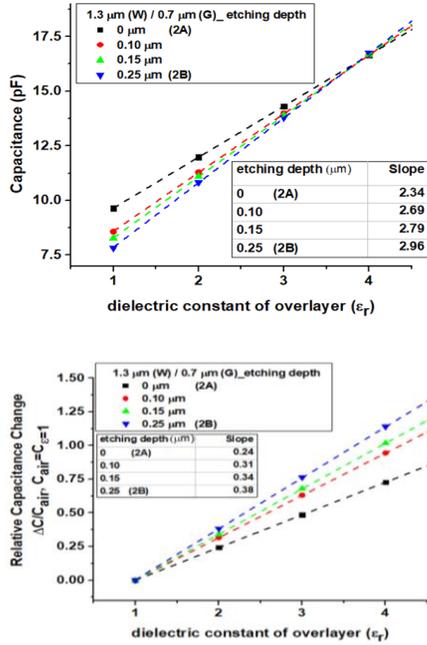

Fig. 6. Calculated capacitance for IDEs with W= 1.3 μm and G= 0.7 μm with aluminum thickness of 120 nm. Examined scenarios for different etching depths of the dielectric substrate as described in the insets. The cases of 2A and 2B are included. (A) Capacitance value vs. dielectric constant of overlayer and (B) relative capacitance change vs. dielectric constant of overlayer.

For these IDEs layouts the sensitivity increases, when the dielectric substrates are etched (slopes in Figs. 5A, 6A). By comparing the results for the 1A and 1B layouts, the sensitivity

increase is calculated to be about 34% (ratio of sensitivities). By applying the same approach, the sensitivity increase is about 27%, as 2A layouts are modified to 2B. Meanwhile, it is observed that the initial capacitance C_{air} is also changed, due to the reduction of the substrate contribution. After the etching process, the sensing overlayer fills the trenches formed between the electrodes. For uncoated etched layouts (configurations: 1B, 2B), the capacitance (C_{air}) is expected to decrease compared to the one for non-etched configurations, due to the smaller dielectric constant of air compared to the SiO_2 substrate (SiO_2: ε_r= 3.9).

Figs. 5A and 6A show that for each one of the IDEs layout cases, when the overlayers have a dielectric constant value equal to that of the SiO_2 substrate (ε_r= 3.9), the capacitance is constant for all etching depth scenarios. This value is depicted as the point of intersection between the different capacitance curves. This is similar to a parallel plate capacitor where all field lines are extended in one material. Above this point, i.e. for coating materials with permittivities higher than the substrate, the capacitance value of the etched sensors will be larger than the unetched ones. Taking into account these capacitance variations of the uncoated sensors (C_{air}), we also present the relative capacitance change, $\Delta C/C_{air}$, (Figs. 5B and 6B). In both cases, etching can induce a relative sensitivity increase up to over 50%.

Additionally, we have considered the variation of the relative sensitivity with the etching depth for the examined IDEs layouts. Simulation results are shown in Fig. 7, where the etching depth is normalized to spatial wavelength, λ. The relative sensitivity increases and saturates for both examined layouts when the etching depth is close to the maximum penetration depth of the electric field i.e. equal to λ/2. The higher maximum relative sensitivity value for IDEs with λ= 8 μm is due to the larger gap between electrodes (G) compared to the electrode width (W), which results in reduced C_{air} values. According to the theoretical study, the optimal etching depth is approximately λ/2. Compared to 1B and 2B cases, simulation predicts that deeper etching up to λ/2 would further increase the relative sensitivity above 40%. It is evident that the spatial wavelength of each IDE layout is crucial, since it constrains both the height of the overlayer, that is sufficient to fully cover the electric field [30], and the maximum beneficial etching depth of the dielectric layer.
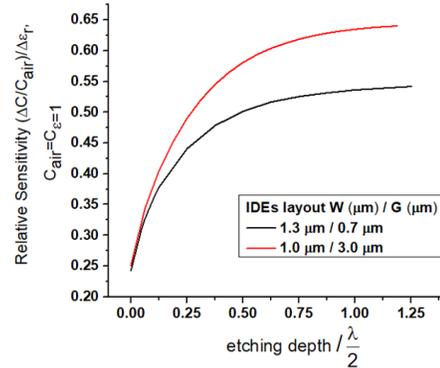

Fig. 7. Theoretical study on the relative sensitivity change vs. the etching depth of the dielectric substrate. X-axis is dimensionless: etching depth / (λ/2).

IV. EVALUATION OF POLYMER-COATED SENSORS

In this work we have chosen to experimentally study cases with intermediate etching depths ($<\lambda/2$) and also investigate their sensing behavior when coated with different polymeric materials. This study is a key aspect for further optimization of the IDEs layout towards the optimum sensing performance. In each case, the sensors were characterized either uncoated or coated with the polymeric materials presented above.

Prior to measurement at gaseous environment of controlled concentration of analytes, the uncoated IDEs were measured in dry environment, upon exposure to inert gas (N_2) and their C_{air} values were compared with those of the theoretical study. In Table IV, the simulation and the experimental data for the various IDEs layouts investigated in the present study are presented. Agreement between the simulation and experimental data is demonstrated for all layouts. For the capacitance measurement, a miniaturized module based on the commercial 24-Bit Capacitance-to-Digital Converter is used [7], that allows for the measurement of capacitance changes of 1fF. The real resistance of IDEs, with DC excitation signal, was measured to be over 100Mohm. In addition, the Q factor of the IDE structures, measured with an HP 4192 LF impedance analyzer at 1MHz, was found to be between 30 and 200. The polymers used as sensing layer are non-conductive, and the real resistance of the final sensors is measured again above 100Mohm.

The polymer coated sensors are tested upon exposure to various concentrations of selected analytes. All measurements were performed with the use of a fully automated, temperature stabilized, set up for the production of constant gaseous environments, by means of the bubbling technique, in continuous flow through the sensors [14]. All analytes were purchased from Sigma Aldrich and used as received. These analytes were: a non-polar solvent (Toluene), a weakly-polar solvent (Ethyl Acetate, EtOAc) and humidity. The capacitance measurements were performed with a previous developed electronics module, that offers a very low noise [14]. Typical dynamic measurements are presented in Figs. 8 and 9.

In Fig. 8 the capacitance changes of same IDEs layouts (2A) coated with different polymer upon exposure to controlled concentrations of humidity and VOCs are presented. In Fig. 9, typical dynamic measurements of sensors with different IDEs layout, and coated with the same polymer are presented. The sensors responses upon exposure to controlled concentration of analyte vapor are defined as $\delta C(fF)=C_{eq}-C_p$, where C_{eq} is the capacitance value in equilibrium with the analyte vapor of a certain concentration (expressed in ppm) and C_p is the capacitance of the polymer coated sensor at dry environment (exposure to N_2).

TABLE IV
COMPARISON BETWEEN SIMULATION AND EXPERIMENTAL DATA FOR SAME IDEs LAYOUTS

IDEs layouts	C_{air} (Simulation values), (pF)	C_{air} (Experimental values), (pF)
1A	4.703	4.546 (±0.229)
1B	3.572	3.619 (±0.139)
2A	9.639	9.626 (±0.395)
2B	7.825	7.729 (±0.255)

TABLE V
SENSITIVITY (MEAN VALUE) OF SELECTED POLYMER-ANALYTE SYSTEMS AND ESTIMATED LIMIT OF DETECTION (LOD)

IDEs	Polymer-Analyte System					
	P(I-S)$_{tap}$-EtOAc		PI-Toluene		PS-Water	
	S (*10^{-3}) fF/ppm	LoD ppm	S (*10^{-3}) fF/ppm	LoD ppm	S (*10^{-3}) fF/ppm	LoD ppm
1A	8.5	118	8.0	125	5.0	200
1B	11.0	91	10.4	96	6.0	167
2A	17.0	59	16.0	62	9.4	106
2B	21.0	48	20.0	50	12.0	83

The response of a chemocapacitive sensor is mainly determined by two factors: (i) the sorption capacity of the polymer to analyte and (ii) the difference in dielectric constants between polymer and analyte. The sorption capacity for a given system is determined by the chemical affinity between polymer and analyte. An estimation of the latter is given by the difference in the solubility parameters, δ, of polymer and analyte. The calculation of solubility parameter for polymer and solvents individually is based on group contribution method [31]. In particular, the estimated values of total solubility parameter δt is 23.5 (cal/cm^3)$^{1/2}$ for water, 13.4 (cal/cm^3)$^{1/2}$ for ethyl acetate and 10.1 (cal/cm^3)$^{1/2}$ for toluene, while for PS and PI are 9.5 and 9.3 (cal/cm^3)$^{1/2}$ respectively.
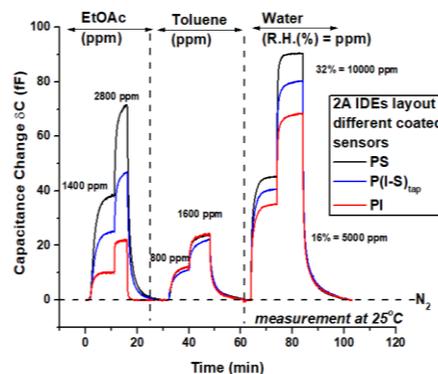

Fig. 8. Dynamic capacitance measurements of same IDEs layouts with different polymer coatings.

Thus, relatively hydrophobic PS and PI materials, are expected to show lower sorption capacity to water, in relation to non-polar toluene and weakly polar ethyl acetate. The higher responses of all sensors to humidity and ethyl acetate vapors in Fig. 8, are due to the higher dielectric constant of these polar molecules as compared to toluene, rather than the sorption capability of the polymeric material to these analytes. Additionally, all three polymer-coated sensors show approximately the same responses to toluene, which is a good solvent for all three polymeric materials. PS shows higher responses to ethyl acetate and water than PI, possibly due to the slightly higher affinity to these analytes or possibly due to excess sorption capacity according to dual mode sorption characterizing glassy polymers. The copolymer shows responses between those of the two homopolymers, in line with mixing rules of composite materials.

TABLE VI
THEORETICAL VS EXPERIMENTAL ESTIMATION OF SENSITIVITY INCREASE

(IDEs on patterned substrate) / (IDEs on planar substrate)	Theoretical sensitivity gain	Experimental sensitivity amplification
S(1B) / S(1A)	1.34	1.26 (±0.05)
S(2B) / S(2A)	1.27	1.25 (±0.03)

For all cases, for sensors coated with the same polymer with different IDEs layouts, (e.g. Fig. 9) an increase in response as λ value of the IDEs is decreased, is observed. Moreover, for all cases with same λ, the responses increase as the substrate is etched.
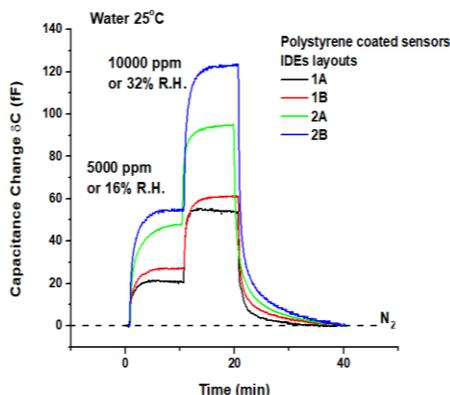

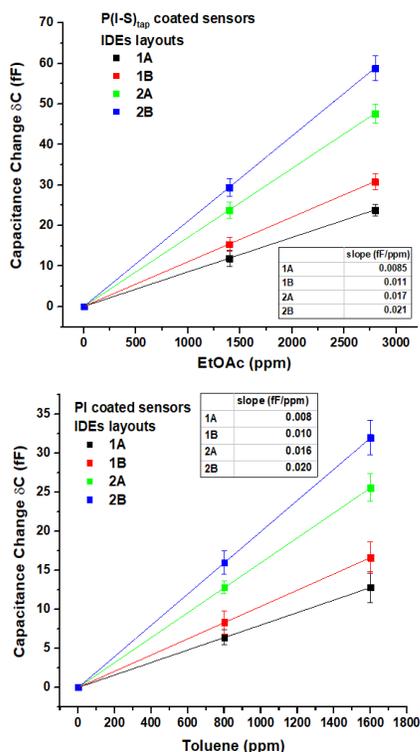Fig. 9. Dynamic measurements of same polymer on different IDEs layouts.

Fig. 10. Plot of equilibrium capacitance change values in relation to various vapor concentrations of (A) EtOAc and (B) toluene, for different IDEs layouts with same polymer coatings (A) P(I-S)tap and (B) PI, respectively.

The responses, were recorded and plotted for different concentrations of the vapor analyte. In Fig.10, the responses for two different polymer-analyte systems for all the examined IDEs layouts are shown. All reported measurements were performed three times in successive days under the same conditions by using the particular measurement set-up that guarantees long term stability of the environmental temperature and humidity. The capacitance responses appear in the related figures, are the mean values of these measurements along with the standard deviation values (Fig. 10). So, the sensors are proved to be reusable in short-term. The excellent recovery of the base capacitance at nitrogen environment is a clear indication of the long term stability of the developed sensors when these sensors are not exposed in environments that modify the polymeric layer properties. Further measurements will be performed in the near future, to study the long-term stability and the aging effect of the sensors.

For all IDEs layouts and polymer-analyte systems, the $\delta C(fF)$ vs. analyte concentration plots were linear. This is due to the low concentration range studied, or in the case of humidity, due to the low sorption capability of the particular polymers. For all polymer- analyte systems the sensitivity $(S=\delta C/ppm \ (fF/ppm))$ is calculated, table V. The measurement noise is $\sim$0.2-0.3 fF [15] and therefore capacitance signal (δC) of 1 fF (Signal/Noise=3) is detectable.

The limit of detection (LoD) is defined per analyte and is the analyte's minimum detectable concentration i.e. the lowest quantity of a substance that can be distinguished from the absence of that substance (nitrogen environment, a blank value). LoD is calculated by linear extrapolation of the ΔC vs. analyte concentration curve to $3\sigma/S$, where σ is the standard deviation of the blank capacitance value, and sensitivity $S=\delta C/ppm \ (fF/ppm))$ is the slope of the fitting curve. The standard deviation of the blank value is the noise of the read-out electronics module employed for the measurement of the sensor response, and in the particular case has a value of 0.2fF-0.3fF [15]. Therefore the LoD(fF) is equal to 1.0fF/S(fF/ppm). For all investigated IDE layouts, the results [mean values of sensitivity S, and LoD] for the three examined polymer-analyte systems are presented in Table V.

The sensitivity of polymer-analyte system increases with the decrease in λ (1A and 2A samples). For the same λ and for each polymer-analyte system the sensitivity increases when the substrate is etched. This is also depicted by the reduction of the LoD values respectively. According to the theoretical study (Fig. 7) the optimal etching depth is λ/2 and the predicted enhancement of LoD would be 15% (i.e. for 1.3 μm (W) / 0.7 μm (G) layouts with substrate etching upon λ/2, the LoD for P(I-S)tap-coated sensor-EtOAc system is estimated to be 41 ppm). The trend of this enhancement is defined by the ratio of the sensitivities for IDEs with and without substrate etching. The experimental results are shown in Table VI together with the theoretical values. The experimental data are presented as mean values with the standard deviation as calculated from the above different polymer analyte systems. The conformity between theoretical and experimental results is fairly good.

V. CONCLUSION

The planar IDEs configuration as a platform for chemocapacitive sensor applications has proven to be a feasible

and low-cost approach, compared to other types of capacitors. In this work, we are dealing with the task of sensitivity increase of sensors with specified electrode width/gap dimensions. In order to address this issue, without distortion of the electrodes configuration, we explore the case of patterning the dielectric substrate with etching technique.

Prior to fabrication, a theoretical study was deemed necessary for determination of the sensing performance of the examined IDEs layouts (with and without substrate patterning). This was realized with Finite Element Simulations by using COMSOL Multiphysics. Two IDE layouts with different λ were systematically studied. For both cases, the theoretical study showed a significant increase in (relative) sensitivity when the etching procedure is realized. A study about the optimum etching depth for each IDEs configuration is also reported.

Selected IDEs layouts (with and without substrate patterning) were fabricated and evaluated. For all cases the agreement between theoretical and experimental results is evident (Table IV). The IDEs were coated with different polymeric materials and measurements upon exposure to analytes of varying polarity were performed. The response of the polymeric materials used was determined by both their sorption capacity and mode of sorption to each analyte, in conjunction with the difference in dielectric constants between polymer and analyte. For all cases of IDEs layouts and polymer-analyte systems, the responses were linear with the concentration of the analytes. The experimental sensitivity of every polymer-analyte system is increased as λ is reduced. Additionally, for layouts with same λ, the sensitivity is increased as the substrate is patterned. This is also expressed in lower LoD values for all polymer-analyte systems. The theoretically estimated trend in sensitivity increase is in accordance with the results of the experimental study.

REFERENCES

[1] A. V. Mamishev, et al., "Interdigital sensors and transducers", Proc. IEEE vol. 92 pp. 808–845, 2004.

[2] C. Hagleitner, A. Hierlemann, D. Lange, A. Kummer, N. Kerness, O. Brand, H. Baltes, "Smart single-chip gas sensor microsystems", *Nature* vol. 414 pp. 293–296 2001.

[3] J.-J. Su, L. Beardslee, O. Brand, "Combined chemoresistive and chemocapacitive microsensor structures", in: 2013 Transducers & Eurosensors XXVII: The 17th International Conference on Solid-State Sensors, Actuators and Microsystems (2013) 258–261.

[4] M. D. Steinberg, I. Žura, I. Murkovic Steinberg, "Wireless smart tag with on-board conductometric chemical sensor", *Sens. Act. B* vol. 196 pp. 208–214, 2015.

[5] U. Altenberend, F. Molina-Lopez, A. Oprea, D. Briand, N. Bârsan, N. F. De Rooij, U. Weimar, "Towards fully printed capacitive gas sensors on flexible PET substrates based on Ag interdigitated transducers with increased stability" *Sens. Act. B* vol. 187 pp. 280– 287, 2013.

[6] A. Rivadeneyra, J. Fernández-Salmerón, M. Agudo-Acemel, J. A. López-Villanueva, A. J. Palma, L. F. Capitan-Vallvey, "A printed capacitive–resistive double sensor for toluene and moisture sensing", *Sens. Act. B* vol. 210 pp. 542–549, 2015.

[7] P. Oikonomou, A. Botsialas, A. Olziersky, E. P. Hadjigeorgiou, S. Katsikas, D. Dimas, G. Sotiropoulos, I. Raptis, M. Sanopoulou, "A self-calibrated Wireless Sensing System for monitoring the ambient industrial environment. From lab to real-time application", *Sens. Act. B* vol. 237 pp. 509–520, 2016

[8] T. E. Mlsna, S. Cemalovic, M. Warburton, S. T. Hobson, D. A. Mlsna, S. V. Patel, "Chemicapacitive microsensors for chemical warfare agent and toxic industrial chemical detection", *Sens. Act. B* vol. 116 pp. 192–201, 2016.

[9] E. Korzeniewska, A. Szczęsny, "Parasitic parameters of thin film structures created on flexible substrates in PVD process", *Microelectron. Eng.* vol. 193 pp. 62–64, 2018.

[10] C. K. Ho, R. C. Hughes, "In-Situ Chemiresistor Sensor Package for Real-Time Detection of Volatile Organic Compounds in Soil and Groundwater", *Sensors* vol. 2 pp. 23-34, 2002.

[11] J. Staginus, I. M. Aerts, Z. Chang, G. C. M. Meijer, L. C. P. M. de Smet, E. J. R. Sudhölter, "Capacitive response of PDMS-coated IDE platforms directly exposed to aqueous solutions containing Volatile Organic Compounds", *Sens. Act. B* vol. 184 pp. 130-142, 2013.

[12] E. L. Tan, W. N. Ng, R. Shao, B. D. Pereles, K. G. Ong, A Wireless, "Passive Sensor for Quantifying Packaged Food Quality", *Sensors* 7 (2007) 1747-1756.

[13] M. E. E. Alahi, S. C. Mukhopadhyay, L. Burkitt, Imprinted polymer coated impedimetric nitrate sensor for real- time water quality monitoring, *Sens. Act. B* 259 (2018) 753-761.

[14] A. Botsialas, P. Oikonomou, D. Goustouridis, Th. Ganetsos, I. Raptis, M. Sanopoulou, "A miniaturized chemocapacitor system for the detection of Volatile Organic Compounds", Sens. Act. B vol. 177, pp. 776-784, 2013.

[15] S. V. Patel, T. E. Mlsna, B. Fruhberger, E. Klaassen, S. Cemalovic, D. R. Baselt, "Chemicapacitive microsensors for volatile organic compound detection", Sens. Act. B vol. 96 pp. 541-553, 2003.

[16] H. Omran, K. N. Salama, Design and fabrication of capacitive interdigitated electrodes for smart gas sensors, 2015 IEEE 3rd International Conference on Smart Instrumentation, Measurement and Applications (ICSIMA) (2015) 1-4.

[17] R. Igreja, C. J. Dias, "Analytical evaluation of the interdigital electrodes capacitance for a multi-layered structure", Sens. Act. A vol. 112 pp. 291–301, 2004.

[18] Y. Feng, J. Hallstedt, Q. Chen, L. Zheng, Y. Huang, "Development and experimental verification of analytical models for printable interdigital capacitor sensors on paperboard", Sensors, 2009 IEEE, Christchurch, (2009) 1034-1039.

[19] P. Oikonomou, A. Botsialas, A. Olziersky, D. Goustouridis, A. Speliotis, I. Raptis, M. Sanopoulou, "Chemocapacitive sensor arrays on Si substrate: towards the hybrid integration with read-out electronics", *Microelectron. Eng.* vol. 119 pp. 11–15, 2014.

[20] R. Blue, Z. Vobecka, P.J. Skabara, D. Uttamchandani, "The development of sensors for volatile nitro-containing compounds as models for explosives detection", *Sens. Actuators B* vol. 176 pp. 534– 542, 2013.

[21] I. Bilican, M. Tahsin Guler, N. Gulener, M. Yuksel, S. Agan, "Capacitive solvent sensing with interdigitated microelectrodes", *Microsyst Technol.* vol. 22 pp. 659–668, 2016.

[22] A. Nag A. I Zia, X. Li, S. C. Mukhopadhyay, J. Kosel, "Novel sensing approach for LPG leakage detection: Part I: Operating Mechanism and Preliminary Results", *IEEE Sensors J.*, vol. 16, pp. 996-1003, 2016.

[23] A. Nag A. I Zia, X. Li, S. C. Mukhopadhyay, J. Kosel, "Novel sensing approach for LPG leakage detection: Part II: Effects of particle size, composition and coating layer thickness", *IEEE Sensors J.*, vol. 16, pp. 1088-1094, 2016.

[24] N. Afsarimanesh, N., S. C. Mukhopadhyay, M. Kruger Smart Sensors, Measurement and Instrumentation vol. 30, pp. 33-44, 2019.

[25] C. Dominguez, J. Muñoz, R. Gonzalez, M. Tudanca, "CHF3-reactive ion etching for waveguides", *Sens. Act. A* vol. 37–38, pp. 779-783, 1993.

[26] P. J. Flory, Principles of Polymer Chemistry, Cornell University Press (1953).

[27] W. J. Koros, D. R. Paul, "CO2 sorption in poly(ethylene terephthalate) above and below the glass transition", *J. Polym. Sci. Part B: Polym. Phys.* vol. 16, pp. 1947-1963, 1978.

[28] N. Hadjichristidis, H. Iatrou, S. Pispas, M. Pitsikalis, Anionic Polymerization: High Vacuum Techniques, *J. Polym. Sci. Part A: Polym. Chem.* vol. 38 pp. 3211-3234, 2000.

[29] D. J. Worsfold, "Anionic Copolymerization of Styrene and isoprene in Cyclohexane", *J. Polym. Sci. Part A: Polym. Chem.* vol. 5 pp. 2783-2789, 1967.

[30] R. Igreja, C. J. Dias, "Dielectric response of interdigital chemocapacitors: The role of the sensitive layer thickness", *Sens. Act. B* vol. 115 pp. 69-78, 2006.

[31] K. L. Hoy, The Hoy tables of solubility parameters, Union Carbide Corp. (1985)

Dr. Petros Oikonomou received the B.Sc. degree in Chemistry from the Chemistry Department of Ioannina University in 2003. He received the M.Sc. and the Ph.D. degree in "Polymers and their Applications" from the Chemistry Department of University of Athens in 2005 and 2012, respectively. Currently, he is working as a Research Fellow at Institute of Nanoscience and Nanotechnology at NCSR "DEMOKRITOS" Greece. His research is focusing on the field of chemical microdevices with emphasis in gas sensing applications. His research interests include microfabrication, polymers, (bio)chem sensing applications and physical chemistry.

Athanasios Botsialas received the B.S. degree in Electronics Engineering from the TEI of Piraeus (2005) and the M.Sc. in Microelectronics from University of Athens (2008). From 2006 he is working as Electronics Engineer at the Institute of Microelectronics, NCSR "DEMOKRITOS" and from 2008 he is working as laboratory associate at the Electronic Engineering Department TEI of Piraeus. Currently, he is a PhD candidate in the Department of Informatics &Telecommunications of University of Athens. His interests include instrumentation development, software development, experimental device characterization, design of data acquisition and automation applications for prototype measurement setups.

Nikos Papanikolaou is director of research at the Institute of Nanoscience and Nanotechnology, NCSR "Demokritos. He received his B.Sc. in Physics in 1991 and his Ph.D. from the University of Athens in 1996. He worked as post-doctoral scientist in the Institut für Festkörperphysik, Forschungszentrum Jülich, during 1997, and 1999-2000, and the University of Halle, during 2001-2002. He continued as a research fellow in the Institute of Materials Science in NCSR "Demokritos", Athens, Greece (2002-2003) and became staff member in 2003. His field of research is theoretical nanotechnology. Currently his work is focused on nanophotonics, metamaterials and plasmonics, as well as elastic wave propagation in the nanoscale and the interaction of light with elastic and spin waves.

Ioannis Kazas holds a M.Sc. degree in Microelectronics from the National and Kapodistrian University of Athens. Main research interests include solid state detectors and associated electronics, for spectroscopic and digital imaging applications.

George Polymeropoulos received his B.Sc. in Materials Science Engineering from the University of Ioannina in Greece in 2009. He completed his M.Sc. (2011) and Ph.D. (2015) in Polymer Chemistry at the University of Ioannina, under the supervision of Prof. A. Avgeropoulos. He is currently a postdoctoral fellow in Catalysis Center, at King Abdullah University of Science and Technology (KAUST), working at the Polymer Synthesis Laboratory under the guidance of Prof. N. Hadjichristidis. His research interests include synthesis of well-defined block copolymers through different polymerization methods and the self-assembly behavior in selective solvents or in bulk.

Konstantinos Ntetsikas graduated from the Department of Materials Science and Engineering (DMSE) of University of Ioannina, Greece, in 2008. He obtained his M.Sc. in 2010 and his Ph.D. (2015) in Polymer Chemistry from the same Department under the guidance of Prof. A. Avgeropoulos. Since 2016, he joined Prof. N. Hadjichristidis' research group as postdoctoral fellow at King Abdullah University of Science and Technology (KAUST). His scientific interests include polymer synthesis by anionic polymerization techniques, morphological and thermal characterization of linear and non-linear block co/terpolymers, nanoimprint lithography and direct self-assembly (DSA) techniques.

Nikos Hadjichristidis is Distinguished Professor of Chemical Sciences at King Abdullah University of Science and Technology, Saudi Arabia and Emeritus Professor at the University of Athens, Greece. His research focuses mainly on the synthesis of novel homopolymers, and copolymers with well-defined complex macromolecular architectures. These polymers are ideal models for checking the theory, understanding and improving the performance of industrial polymers and are potential candidates for high-tech applications. He has received several awards including: The Macro Group United Kingdom Medal for Outstanding Achievements (2016); The ACS National Award for Polymer Chemistry (2015); the ACS, Rubber Division Chemistry of Thermoplastic Elastomers Award (2011); The ACS, Polymeric Materials Science and Engineering (PMSE) Division Cooperative Research Award (2010); The International Award of the Society of Polymer Science, Japan (SPSJ, 2007). He is the author of more than 500 articles in peer-reviewed international journals and holder of more than 30 patents.

Dr. Merope Sanopoulou received her B.Sc. degree in Chemistry from the University of Athens in 1977 and her Ph.D. in Physical Chemistry from the same institution in 1984. She then joined the Institute of Physical Chemistry, NCSR "DEMOKRITOS", currently being Head of the Laboratory of Transport of Matter Phenomena in Polymers. She has been engaged in extensive modeling and experimental studies of sorption and diffusion in polymer films. She is the author/co-author of more than 70 publications in peer-reviewed journals and has been key researcher/leader in various National and EU research projects.

Ioannis Raptis received his Ph.D. on e-beam lithography (1996) from the University of Athens. Since 2003 he works at NCSR"DEMOKRITOS" as researcher, and since 2013 as a Director of Research on the implementation of technologies and electronic/photonic devices in the micro/nano scale for bio/chemical sensing applications. He is/was Key Researcher and Coordinator of several EU and national funded research projects. He is author of more than 150 articles in peer-reviewed international journals and holder of 5 patents.